Materials Chemistry and Physics 223 (2019) 32–38

Contents lists available at ScienceDirect

Materials Chemistry and Physics

journal homepage: www.elsevier.com/locate/matchemphys

3-Mercaptopropionic acid functionalization of titanium dioxide thin films

Orisson P. Gomes[a,b], Nilton F. Azevedo Neto[a], Erika S. Bronze-Uhle[a,b], Luciana D. Trino[a,b], Cássio M. dos Santos[a,b], José H.D. da Silva[a], Paulo N. Lisboa-Filho[a,b,*]

[a] UNESP - Univ Estadual Paulista, Departamento de Física, Av. Eng. Luiz Edmundo Carrijo Coube 14-01, 17033-360, Bauru, SP, Brazil
[b] Brazilian-Branch of the Institute of Biomaterials, Tribocorrosion and Nanomedicine, Bauru, SP, Brazil

HIGHLIGHTS

- Nanostructured titanium dioxide films are commonly employed as surface modifiers.
- Monophasic anatase and rutile TiO2 films were grown onto Ti substrates.
- The surfaces of these oxides are mainly terminated by -OH groups.
- The -OH groups can be readily functionalized by bifunctional molecules.
- The functionalization with MPA was seen to occur only for the rutile phase.

ARTICLE INFO

Keywords:
Surface functionalization
Biomaterials
X-ray photoelectron spectroscopy
Thin films

ABSTRACT

Nanostructured titanium dioxide (TiO_2) films are commonly employed as surface modifiers on medical and dental metallic implants, presenting promising results related to interactions with living tissues, promoting improvements in the *in vivo* biocorrosion resistance and increased bioactivity when compared to non-coated metallic materials. In addition to these properties, titanium dioxide is also well recognized for its biocompatibility. However, considering the necessary integration with surrounding tissues when this oxide is applied as implant coatings, there are many aspects of the adhesion mechanisms located at the interface between the biological environment and the oxide surface that still need to be addressed. Specifically regarding the surface chemistry, these oxides are mainly terminated by hydroxyl groups (-OH) that are readily functionalized by different molecules, such as the 3-mercaptopropionic acid (MPA). In this contribution, X-ray photoelectron spectroscopy (XPS) and atomic force microscopy (AFM) were used to examine the adsorption of MPA on anatase- and rutile-phase forms of TiO_2 thin film surfaces grown by RF magnetron sputtering. According to the obtained results, both anatase and rutile TiO_2 films present similarities in roughness and thickness. However, different responses to interaction with the MPA molecules were observed, wherein the functionalization was seen to occur only for the rutile phase.

1. Introduction

Titanium and its alloys are extensively used in the fields of medicine and dentistry. As biomaterials, in particular, they have a wide range of applications ranging from bone anchorage devices to dental implants and prostheses to replacement joints, including cardiac devices, such as heart valves [1]. Although these materials exhibit good mechanical properties, their surficial, thin, native oxide layers (5–6 nm) are incapable of protecting them from long-term corrosion [2–4]. Furthermore, Werner et al. [5] found that this native, oxide layer is generally less hemocompatible compared to the thicker and more homogeneous layer of titanium dioxide (TiO_2). Other studies have shown that the crystallinity, thickness, and porosity of titanium films relate to the phenomenon of bone tissue integration, and the deposition of nanometric-phase titanium films on stainless steel results in better adhesion and proliferation of osteoblasts [6–8]. In view of this, nanostructured TiO_2 has been studied for its use in several biomedical applications, as semiconductor nanomaterials, anticancer drug transporters, and biomedical implants [3,9–11].

Nanostructured TiO_2 has been used in several studies as a surface modifier because it presents high hardness, increased dielectric constant, and very good chemical stability [12–14]. Surface modification with TiO_2 can promote an improvement in the biocorrosion resistance of materials and increase oxide bioactivity, which presents promising

* Corresponding author. UNESP - Univ Estadual Paulista, Departamento de Física, Av. Eng. Luiz Edmundo Carrijo Coube 14-01, 17033-360, Bauru, SP, Brazil.
E-mail address: paulo.lisboa@unesp.br (P.N. Lisboa-Filho).

https://doi.org/10.1016/j.matchemphys.2018.10.041
Received 23 May 2018; Received in revised form 6 October 2018; Accepted 21 October 2018
Available online 22 October 2018
0254-0584/ © 2018 Elsevier B.V. All rights reserved.

Table 1
Deposition parameters used to obtain anatase and rutile phases [35].

	Substrate holder temperature (°C)	Oxygen flow (sccm)	Argon flow (sccm)	RF power (W)	Pressure (Pa)	Deposition time (min)
TiO_2 Anatase	200	1.0	40.0	240	4.0	1440
TiO_2 Rutile	600	4.0	40.0	290	0.3	720

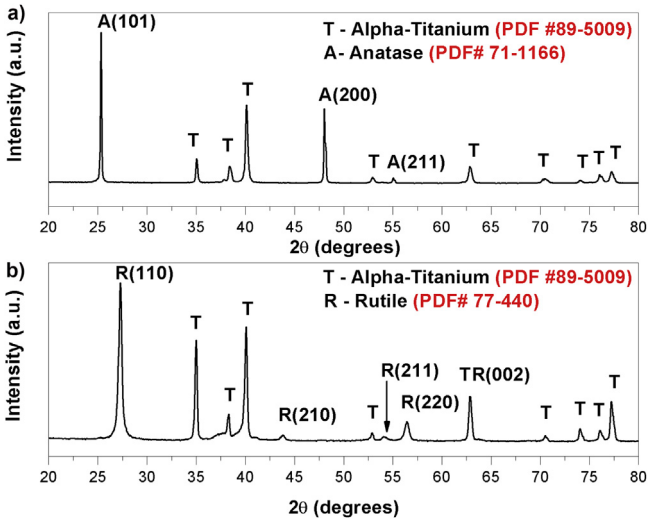

Fig. 1. a) X-ray diffraction pattern of the anatase TiO_2 sample. b) X-ray diffraction pattern of the rutile TiO_2 sample.

results for interaction with tissue since biocompatibility is determined by chemical processes that occur at the interface between an implant and proteins in biological fluids [9]. Although the biocompatibility of these oxides has been recognized, more study is required to understand the adhesion mechanisms of these proteins. Various *in vitro* and *in vivo* assays have been performed to evaluate the biological responses of metal oxide coatings and demonstrate that the biocompatibility and biocorrosion properties depend on the composition, thickness, homogeneity, and porosity of the material [15].

Chemically, the oxide surface is mainly terminated by -OH groups, which can be readily functionalized by various bifunctional molecules, such as carboxylic acids and other derivatives, like esters, acid chlorides, carboxylate salts, and others, by forming self-assembled monolayers (SAMs) on the oxide surface. These derivatives form covalent bonds with the oxide through reactions with the hydroxyl groups on the TiO_2 surface [16]. This hydroxylated surface can be dissociated into solution and generate positive, negative, or neutral charges depending on the pH [5,17–20]. The chemical functionalization or physical modification of this material surface can improve the oxide's interaction with the biological environment because, depending on the functionalization, this material can dissolve in both acidic and basic environments [5]. Consequently, interactions among metal oxides, proteins, and cells are governed by the chemical and physical properties of the corresponding metal oxides under study [11]. SAMs have well-defined surface properties, such as uniformity, stability, and reproducibility, which alter the adsorption of proteins on functionalized surfaces.

TiO_2 films can be prepared on commercial, pure titanium Grade IV (Ti CP4) surfaces by various methods [21]. These methods include sol-gel processes [22], ion beams [23], reactive sputtering [24,25], electron beam evaporation [26], chemical vapor deposition [27–29], among others. All these methods lead to the formation of different crystalline structures and morphologies. Consequently, the crystallinity and morphology of the films' surfaces strongly depend on the method and the preparation conditions employed. Among these, the RF magnetron sputtering deposition method provides precise control over the composition and morphology of the surface by adjusting the conditions of deposition. TiO_2 properties depend strongly on the microstructure and crystallographic phase (rutile or anatase) obtained. In general, films are formed with high uniformity, density, adhesion, and hardness, which make them attractive for use in biomedical implants. For example, anatase-phase films exhibit high photocatalytic activity while rutile-phase films exhibit high refractive indices [5]. Nevertheless, the physical and chemical properties of the TiO_2 anatase phase formed on metallic surfaces are poorly understood.

In the current study, anatase and rutile TiO_2 films were deposited on a Ti CP4 surface by RF magnetron sputtering. The adsorption of 3-mercaptopropionic acid $[HS(CH_2)_3COOH]$ (MPA) onto the TiO_2 film

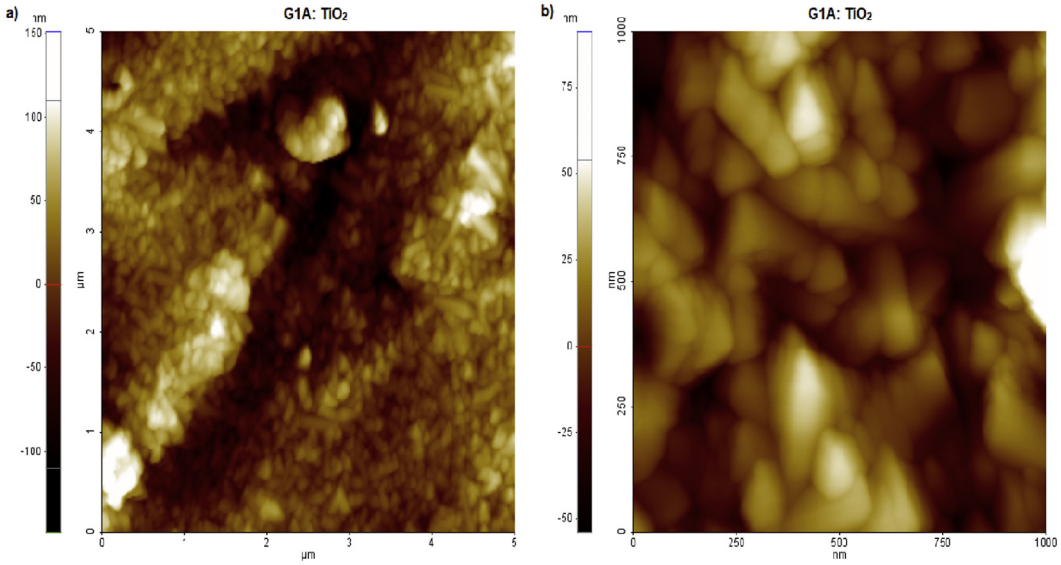

Fig. 2. AFM image showing the surface of an anatase sample of the control group, G1A. a) scan size of 5 µm × 5 µm, b) scan size of 1 µm × 1 µm.

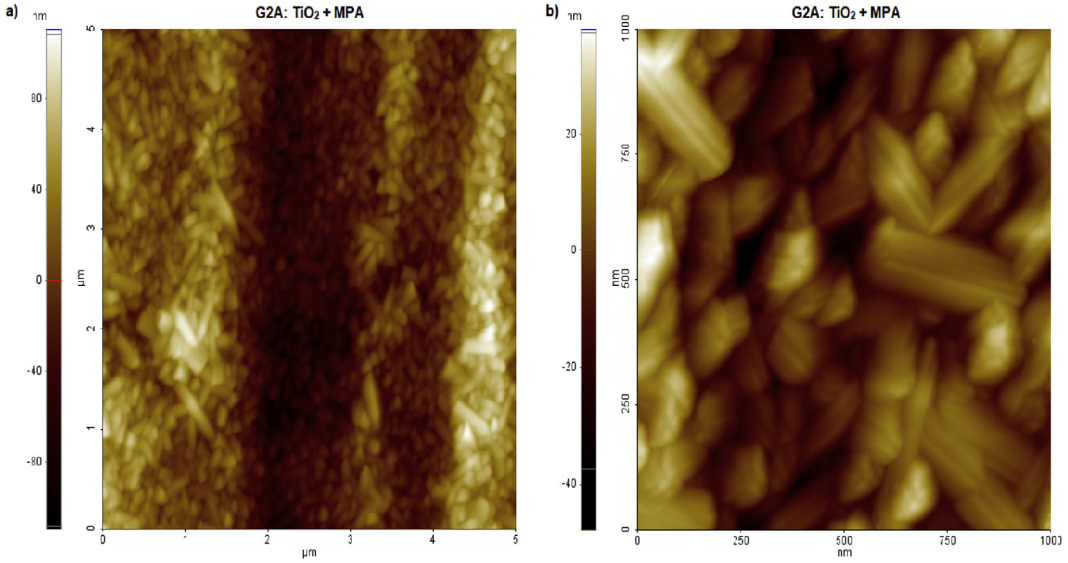

Fig. 3. AFM image showing the surface of an anatase sample immersed in a 3 mM (pH 3) MPA solution, G2A. a) scan size of 5 µm × 5 µm, b) scan size of 1 µm × 1 µm.

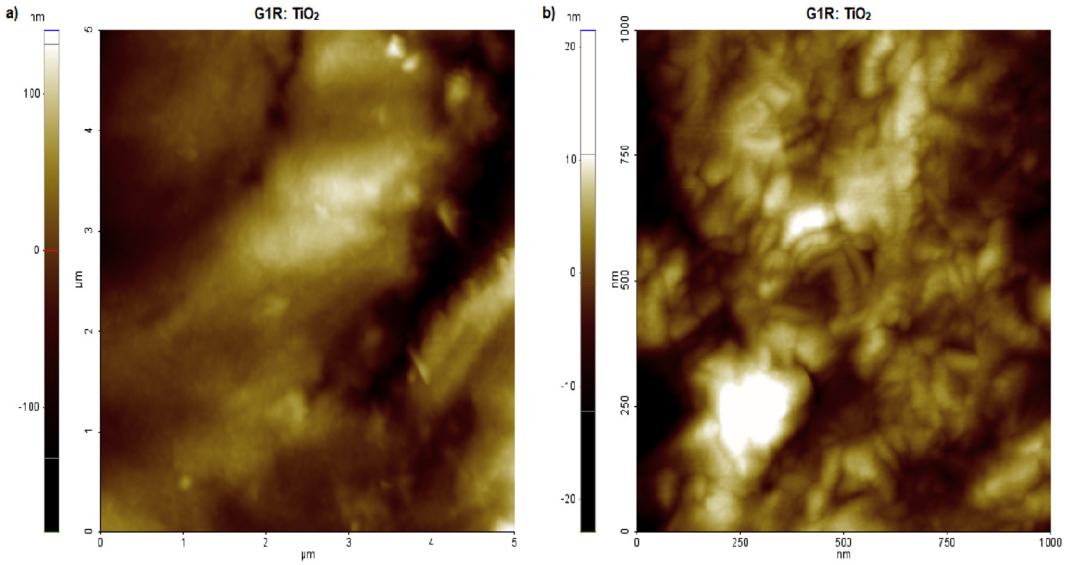

Fig. 4. AFM image showing the surface of a rutile sample of the control group, G1R. a) scan size of 5 µm × 5 µm, b) scan size of 1 µm × 1 µm.

was performed by means of a SAM of molecules from solution. MPA SAMs have been studied as surface modifiers for biomedical applications and utilized for attaching peptides [30], proteins [31], and DNA [32]. The crystalline phase, morphology, and roughness of the pristine TiO_2 films and those functionalized with MPA were analyzed using x-ray diffraction (XRD) and atomic force microscopy (AFM). The surfaces' chemical characteristics were evaluated using x-ray photoelectron spectroscopy (XPS).

2. Experimental

Due to its extensive use in different kinds of implants [1], pure titanium was chosen as the preferential substrate for this analysis. Ti CP4 substrates were sequentially wet-sanded with 320, 400, 600, and 800-grit mesh sandpapers. To remove any impurities, the substrates were then washed in an ultrasonic bath with deionized (DI) water and isopropanol; they were then washed with DI water for 10 min. The Ti CP4 substrates were then etched and hydroxylated for two hours in order to remove any remaining traces of sandpaper and native oxide layers. This process was carried out using a 3:7 (volume) piranha solution of H_2O_2 and H_2SO_4, respectively. Finally, the substrates were immersed in an ultrasonic bath for a total of 40 min (30 min in deionized water and 10 min in isopropanol).

The TiO_2 films, present as anatase and rutile phases, were deposited onto the prepared metallic titanium substrates, described above, using an RF reactive magnetron sputtering system (Kurt J. Lesker). Table 1 shows the deposition parameters that were used to obtain both phases. Oxygen and argon gases (6 N purity) were used for this deposition. A titanium target of 99.999% purity with a 3 mm diameter was used (AJA International). After the deposition process, the samples were divided into four groups: two control groups with only TiO_2 films on the Ti CP4 substrates (sample G1A for anatase and sample G1R for rutile) and two groups immersed in a 3 mM ≥ 99% MPA (Sigma-Aldrich) solution (pH 3) for one hour (sample G2A for anatase and sample G2R for rutile) and then washed in deionized water [33,34].

X-ray diffraction measurements using a diffractometer (MiniFlex 600; Rigaku Corp.) were made using Bragg–Brentano geometry in the range of 20°–80° with a scan speed of 10°/min and a step of 0.04°. CuKα

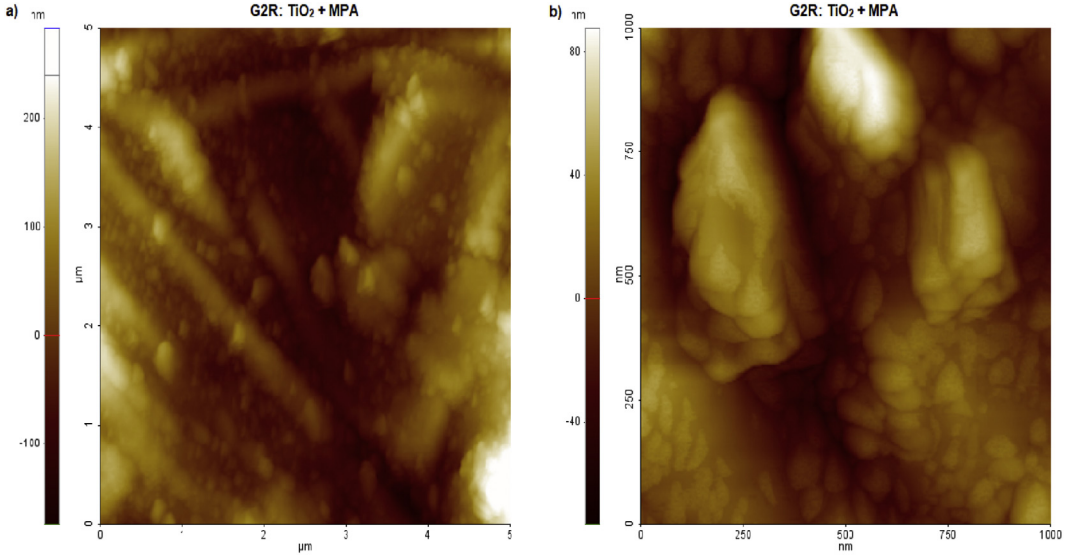

Fig. 5. AFM image showing the surface of an anatase sample immersed in a 3 mM (pH 3) MPA solution, G2R. a) scan size of 5 µm × 5 µm, b) scan size of 1 µm × 1 µm.

Table 2
Contact angles of all samples and their respective pictures.

Sample	Contact Angle (º)	Image
G1A	44.8 ± 1.7	
G2A	34.2 ± 0.7	
G1R	68.6 ± 3.3	
G2R	43.6 ± 2.9	

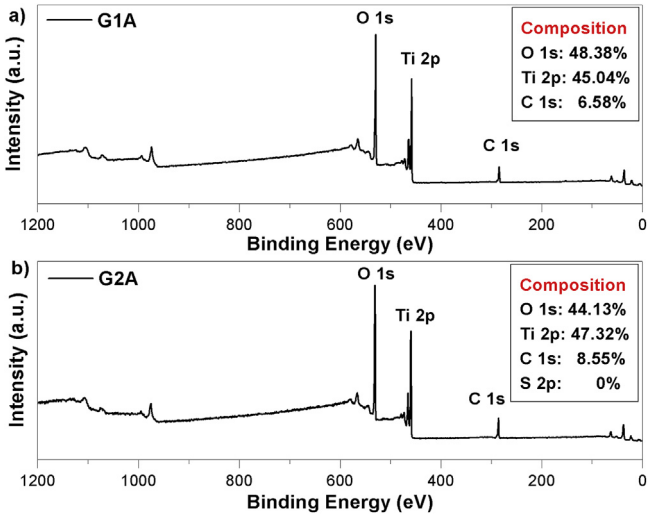

Fig. 6. XPS survey spectra of a) G1A and b) G2A.

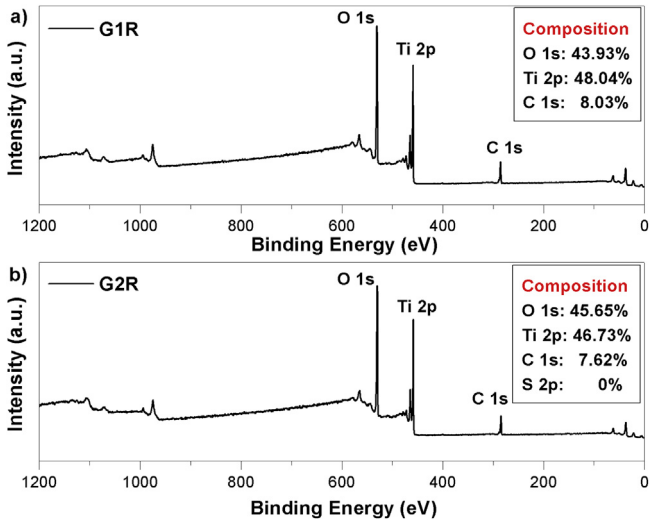

Fig. 7. XPS survey spectra of a) G1R and b) G2R.

radiation (λ = 1.54056 Å) with 8.06 keV energy was used, and the equipment was operated at 40 kV and 15 mA. AFM for the qualitative surface investigation was made in non-contact mode (Park XE7; Park Systems).

Reflectance measurements were measured in the 250–2500 nm range using a spectrophotometer (Lambda 1050; PerkinElmer Inc.). The thickness of the films was determined using optical interference fringes based on Cisneros' method [36].

XPS analysis used a monochromatic Al Kα x-ray source (Kratos AXIS-165). Each sample was analyzed at a takeoff angle of 54.7°, defined as the angle of emission relative to the surface; the energy resolution was 0.45 eV. Survey scan spectra and individual high-resolution spectra were recorded with pass energies of 80 eV and 20 eV, respectively. To correct for any charging effect, the binding energy of the C 1s peak was normalized to 284.8 eV. Curve fitting was performed using CasaXPS software.

3. Results and discussion

XRD analyses of the as-grown TiO_2 films are shown in Fig. 1; the films showing anatase and rutile phases are shown in Fig. 1a and b,

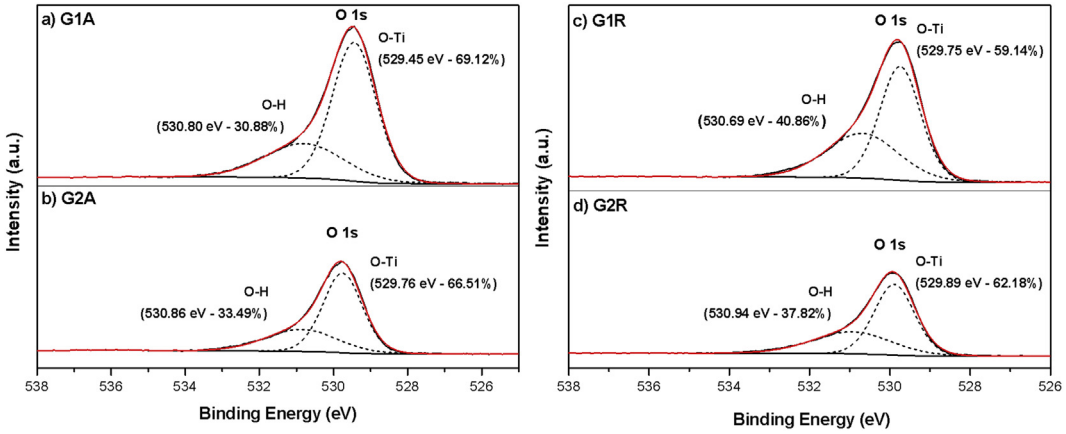

Fig. 8. XPS spectra of O 1s peak of anatase a) G1A, b) G2A, and rutile c) G1R, d) G2R groups.

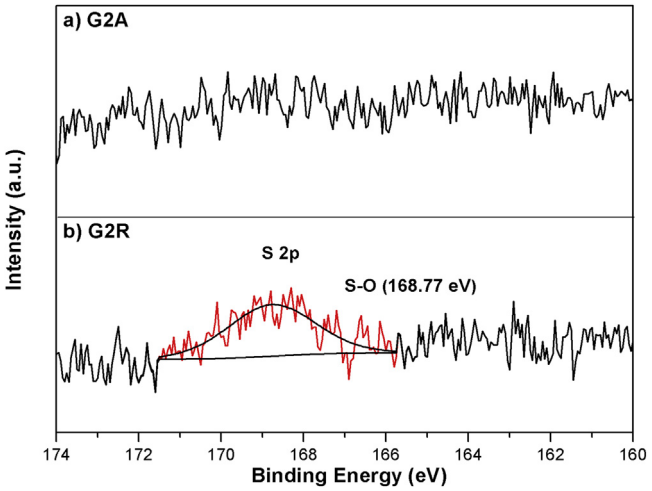

Fig. 9. XPS spectra of S 2p peak of anatase a) G2A and rutile b) G2R groups.

respectively. Both patterns presented different intensities and orientations, which indicated that the anatase- and rutile-phase films were polycrystalline. It was also possible to observe alpha-titanium peaks (labeled T) for both samples. The optically measured thicknesses were 1049 (± 5%) nm and 738 (± 5%) nm for anatase and rutile, respectively. Since the penetration depth of 8.06 keV CuKα radiation into titanium is around 19.90 μm and the substrate is titanium, the presence of metallic titanium in both diffraction patterns was, accordingly, consistent [37].

A qualitative surface investigation was made using non-contact mode AFM to study variations in topography. Figs. 2–5 show the G1A, G2A, G1R, and G2R samples' topographies, respectively, with scan sizes of a) 5 μm and b) 1 μm. From the AFM images, it was possible to observe differences in the rutile's and anatase's morphologies (G1 group). TiO_2 films in anatase phase presented better uniformity of grain size and morphology while rutile-phase films presented non-uniform patterns. Both the anatase and rutile particle samples exhibited better definition after immersion in MPA solution; this difference might have been related to the presence of MPA on the material surface. This improvement could have been the result of better interaction between the probe and the sample surface [38].

Hypothetically, the MPA molecules might have taken the place of the contaminant molecules (such as CO_2) in an energetically favorable reaction, or these contaminants were washed away during the synthesis process, leaving the surface cleaner than before. As a bifunctional group, the MPA could have increased the superficial energy and, consequently, enhanced the interaction between the probe and the surface. Complementary to this hypothesis, contact angle measurements using water were carried out on all samples to investigate variations in wettability (Table 2). For the G1 group, it was possible to observe that the anatase phase presented higher wettability than the rutile phase. However, after the immersion process, the contact angle of the rutile phase decreased from 68.6° ± 3.3° to 43.6° ± 2.9° while the anatase phase presented a smaller decrease, from 44.8° ± 1.7° to 34.2° ± 0.7°. The surface roughness was analyzed by confocal microscopy, and the results showed a root mean square equal to 155 (± 3) nm for the substrate after sanding; this was 167 (± 12) nm for the G1A sample and 188 (± 7) nm for the G1R sample. It was clear that the anatase

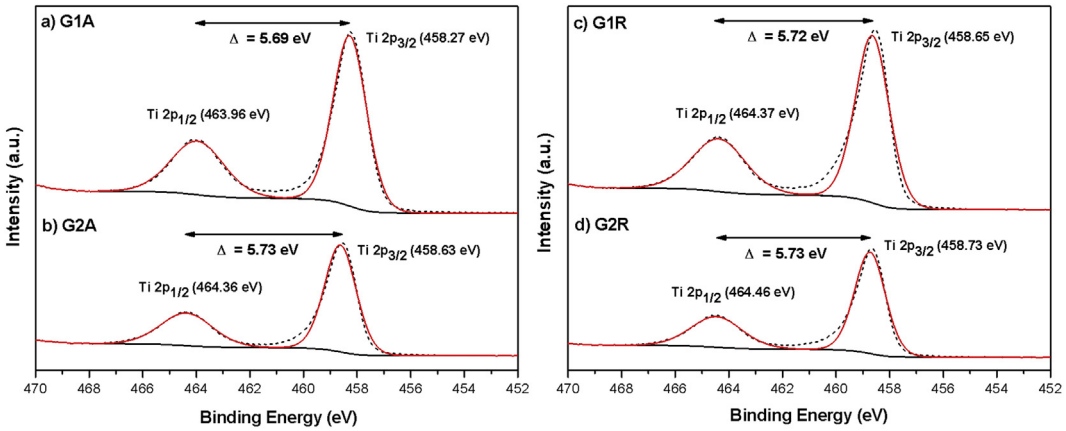

Fig. 10. XPS spectra of Ti 2p peaks of anatase a) G1A, b) G2A, and rutile c) G1R, d) G2R groups.

phase had higher wettability, even with a small surface roughness. In addition, the rutile phase was more affected by the MPA functionalization process.

Representative XPS survey spectra of the anatase- and rutile-phase groups are shown in Figs. 6 and 7, respectively, and the elemental compositions of the samples' surfaces are indicated. It was possible to observe the presence of carbon even in the control groups, which can be related to organic contamination. It is relevant to emphasize that the variations were relatively small and below the accuracy of 10% typically quoted for routinely performed XPS atomic concentrations [39].

The O 1s spectra of the control and functionalized samples are shown in Fig. 8. The O 1s spectrum for the G1A sample revealed two contributions; the major one at 529.5 eV referred to the Ti-O bonding of the TiO_2 and the second contribution at higher energy (530.8 eV) was related to O-H bonding. This indicated the presence of hydroxyl groups on the TiO_2 surface, which could have acted as binding sites for MPA adhesion. For the G2A sample, there was a contribution at 530.9 eV, which could have also been related to the O-H bonding.

The S 2p spectra of the functionalized G2A and G2R samples are shown in Fig. 9. No signal was detected for the G2A sample and a contribution at 168.77 eV was detected for G2R; this contribution was related to S-O-Ti bonding. The weak signal of sulfur for G2R suggested a monolayer-like pattern of MPA molecules. The carbon adsorbed from the contamination was likely desorbed and substituted by MPA molecules during the immersion process. This substitution was seen to be energetically favorable for the rutile phase compared to the anatase phase. It is important to note that both the anatase and rutile exhibited acidic behavior when immersed in an MPA solution of pH because the point zero charges of these phases were 6.2 and 5.3, respectively [4].

The Ti 2p spectra for all the groups are shown in Fig. 10. The difference between the Ti $2p_{1/2}$ and Ti $2p_{3/2}$ peaks was approximately 6 eV, which was consistent with the Ti^{4+} oxidation state from the bound TiO_2, even after immersion in the MPA solution.

The two polymorphic forms of TiO_2, rutile and anatase, are known to present physicochemical and photocatalytic differences, although the processes involved are not well elucidated. Studies have shown that in photoactivated reactions, active oxygen species generated by electrons and holes such as OH radicals, superoxide radicals, and hydrogen peroxide are formed on these oxide surfaces [40]. The generation of OH radicals is reported to be responsible for the oxidation of organic compounds initiated by heterogeneous photocatalytic processes. According to Kakuma et al. [41], the process is more recurrent on anatase surfaces when compared to rutile. The explanation lies in the distance between the adjacent titanium atoms in these polymorphic structures. It is discussed that the distance between the two titanium atoms in rutile phase is 296 pm, while in anatase surface is 379 pm. Since the O-O bond length is 146 pm and Ti-O-O- has an angle of 109°, it is difficult to form the Ti-O-O-Ti structure on the anatase surface. On the other hand, the short separation between the adjacent Ti atoms for rutile phase may form the Ti-O-O-Ti dimer, which is not active for the oxidation of organic compounds. Thus, the anatase surfaces do not form the dimer and release OH radicals in the process that promote the oxidation of compounds in solution. In addition, TiO_2 reacts by adsorbing organic molecules on its surface, by electron-hole transfer. Peter et al. [42], proposed that rutile surfaces in the presence of electron donating molecules trigger an immediate reaction between them. Considering the present study of MPA adsorption on different TiO_2 surfaces, non-functionalization of anatase surface may be associated to the oxidation of this compound in aqueous solution during immersion process while in rutile phase the functionalization may be explained by the reaction of Ti-O-O-Ti dimer and MPA molecule, since this compound can donate electrons.

Despite the photocatalytic process of anatase phase is known to present greater efficiency under ultraviolet light, this phenomenon may also occur with a smaller efficiency under ambient light. Therefore, the high catalytic activity of anatase promotes a difficult adsorption of organic compounds on its surface that competes with other physicochemical processes in solution and the washing process may have easily removed the possibly degraded MPA on anatase surface, whereas on the rutile surface this did not occur.

In addition, if this process occurs, there also is an increase in the surface energy of anatase surface. Consequently, this surface will present a lower contact angle, corroborating with the obtained results. In short, while the lower contact angle presented by G2A can be related to the photoactivated surface, the lower contact angle presented by G2R might be related to the presence of MPA molecules.

4. Conclusion

By changing the deposition parameters of the RF magnetron sputtering, it was possible to grow monophasic anatase and rutile films on the top of Ti substrates. AFM results determined the differences in morphology and grain size related to the anatase and rutile phases. Both the G2A and G2R samples exhibited better AFM image definitions and higher wettability, as shown by the contact angle results.

Although the similarities of roughness and thickness, the anatase and rutile phases presented different responses to interaction with the MPA molecules, where the functionalization was seen to occur only for the rutile phase (for this concentration and pH of the MPA solution). In our experiments, presence of MPA molecules was confirmed by XPS analysis to have bound on the titanium surface only for the rutile phase.

Acknowledgments

We would like to thank the FAPESP (2016/22186-7 and 2014/20471-0) and the CEPID (2013/07296-2) for providing financial support.

References

[1] K. Cai, M. Müller, J. Bossert, A. Rechtenbach, K.D. Jandt, Surface structure and composition of flat titanium thin films as a function of film thickness and evaporation rate, Appl. Surf. Sci. 250 (2005) 252–267.
[2] H. Hong, et al., Cancer-targeted optical imaging with fluorescent zinc oxide nanowires, Nano Lett. 11 (2011) 3744–3750.
[3] P. Silva-Bermudez, S. Muhl, S.E. Rodil, A comparative study of fibrinogen adsorption onto metal oxide thin films, Appl. Surf. Sci. 282 (2013) 351–362.
[4] T. Hanawa, A comprehensive review of techniques for biofunctionalization of titanium, J. Periodontal Implant Sci. 41 (2011) 263–272.
[5] F.M. Maitz, U. Freudenberg, M.V. Tsurkan, M. Fischer, T. Beyrich, C. Werner, Bioresponsive polymer hydrogels homeostatically regulate blood coagulation, Nat. Commun. 4 (2013) 2168.
[6] Y.T. Sul, et al., The roles of surface chemistry and topography in the strength and rate of osseointegration of titanium implants in bone, J. Biomed. Mater. Res. 89 (2009) 942–950.
[7] Y.T. Sul, et al., Oxidized implants and their influence on the bone response, J. Mater. Sci. Mater. Med. 12 (2001) 1025–1031.
[8] J.S. Shah, et al., The role of nanocrystalline titania coating on nanostructured austenitic stainless steel in enhancing osteoblasts functions for regeneration of tissue, Mater. Sci. Eng. C 31 (2011) 458–471.
[9] Q. Li, et al., The incorporation of daunorubicin in cancer cells through the use of titanium dioxide whiskers, Biomaterials 30 (2009) 4708–4715.
[10] H. Zhang, et al., A strategy for ZnO nanorod mediated multi-mode cancer treatment, Biomaterials 32 (2011) 1906–1914.
[11] H. Hong, et al., Cancer-targeted optical imaging with fluorescent zinc oxide nanowires, Nano Lett. 11 (2011) 3744–3750.
[12] B. YU, K.M. Leung, Q. Guo, W.M. Lau, J. Yang, Synthesis of Ag–TiO2 composite nano thin film for antimicrobial application, Nanotechnology 22 (2011) 1–9.
[13] V. Zorba, X. Chen, S.S. Mao, Superhydrophilic TiO2 surface without photocatalytic activation, Appl. Phys. Lett. 96 (2010) 1–3.
[14] H.S. Chen, S.H. Huang, T.P. Perng, Highly transparent hard bio-coating synthesized by low temperature sol–gel process, Surf. Coating. Technol. 233 (2013) 140–146.
[15] A. Kumari, S.K. Yadav, S.C. Yadav, Biodegradable polymeric nanoparticles based drug delivery systems, Colloids Surf., B 75 (2010) 1–18.
[16] J.C. Love, et al., Self-assembled monolayers of thiolates on metals as a form of nanotechnology, Chem. Rev. 105 (2005) 1103–1169.
[17] G.D. Parfitt, The surface of titanium dioxide, Prog. Surf. Membr. Sci. 11 (1976) 181–226.
[18] J. Westall, H. Hohl, A comparison of electrostatic models for the oxide/solution interface, Adv. Colloid Interface Sci. 12 (1980) 265–294.
[19] T.W. Healy, D.W. Fuerstenau, The oxide-water interface-interrelation of the zero point of charge and the heat of immersion, J. Coll. Sci. 20 (1965) 376–386.

[20] H.P. Boehm, Acidic and basic properties of hydroxylated metal oxide surfaces, Discuss. Faraday Soc. 52 (1971) 264–275.
[21] C.H. Wei, C.M. Chang, Polycrystalline TiO2 thin films with different thicknesses deposited on unheated substrates using RF magnetron sputtering, Mater. Trans. 52 (2011) 554–559.
[22] M.S. Park, M. Kang, The preparation of the anatase and rutile forms of Ag–TiO2 and hydrogen production from methanol/water decomposition, Mater. Lett. 62 (2008) 183–187.
[23] P.J. Martin, Ion-based methods for optical thin film deposition, J. Mater. Sci. 21 (1986) 1–25.
[24] E. Kusando, A. Kinbara, Time-dependent O2 mass balance change and target surface oxidation during mode transition in Ti-O2 reactive sputtering, J. Appl. Phys. 87 (2000) 2015–2019.
[25] L. Meng, M. Andritschky, M.P. dos Santos, The effect of substrate temperature on the properties of dc reactive magnetron sputtered titanium oxide films, Thin Solid Films 223 (1993) 242–247.
[26] C. Yang, et al., Effects of depositing temperatures on structure and optical properties of TiO2 film deposited by ion beam assisted electron beam evaporation, Appl. Surf. Sci. 254 (2008) 2685–2689.
[27] L.M. Williams, D.W. Hess, Structural properties of titanium dioxide films deposited in an rf glow discharge, J. Vac. Sci. Technol., A 1 (1983) 1810–1819.
[28] D.J. Won, et al., Effects of thermally induced anatase-to-rutile phase transition in MOCVD-grown TiO2 films on structural and optical properties, Appl. Phys. A 73 (2001) 595–600.
[29] M. Nakamura, et al., Hydrophilic properties of hydro-oxygenated TiOx films prepared by plasma enhanced chemical vapor deposition, Surf. Coating. Technol. 169–170 (2003) 699–702.
[30] L.D. Trino, E.S. Bronze-Uhle, A. Ramachandran, P.N. Lisboa-Filho, M.T. Mathew, A. George, Titanium surface bio-functionalization using osteogenic peptides: surface chemistry, biocompatibility, corrosion and tribocorrosion aspects, J. Mech. Behav. Biomed. Mater. 81 (2018) 26–38.
[31] J.H. Li, G.J. Cheng, S.J.J. Dong, Direct electron transfer to cytochrome c oxidase in self-assembled monolayers on gold electrodes, Electroanal. Chem. 416 (1996) 97–104.
[32] Y.D. Zhao, D.W. Pang, S. Hu, Z.L. Wang, J.K. Cheng, H.P. Daib, DNA-modified electrodes; part 4: optimization of covalent immobilization of DNA on self-assembled monolayers, Talanta 49 (1999) 751–756.
[33] M. Advincula, X. Fan, J. Lemons, R. Advincula, Surface modification of surface sol–gel derived titanium oxide films by self-assembled monolayers (SAMs) and non-specific protein adsorption studies, Colloids Surf., B 42 (2005) 29–43.
[34] M.C. Martins, B.D. Ratner, M.A. Barbosa, Protein adsorption on mixtures of hydroxyl- and methylterminated alkanethiols self-assembled monolayers, J. Biomed. Mater. Res. 67 (2003) 158–171.
[35] S. Mráz, J.M. Schneider, Structure evolution of magnetron sputtered TiO2 thin films, J. Appl. Phys. 109 (2011).
[36] J.I. Cisneros, Optical characterization of dielectric and semiconductor thin films by use of transmission data, Appl. Opt. 37 (1998) 5262–5270.
[37] M. Birkholz, Thin Film Analysis by X-Ray Scattering, WILEY-VCH Verlag GmbH & Co, Weinheim, BW, 2006.
[38] D. Buckley, Surface Effects in Adhesion, Friction, Wear, and Lubrication, Elsevier, Netherlands, 2000.
[39] N. Fairley, CasaXPS.
[40] J. Zhang, Y. Nosaka, Photocatalytic oxidation mechanism of methanol and the other reactants in irradiated TiO_2 aqueous suspension investigated by OH radical detection, Appl. Catal. B Environ. 166–167 (2015) 32–36.
[41] Y. Kakuma, A.Y. Nosaka, Y. Nosaka, Difference in TiO2 Photocatalytic mechanism between rutile and anatase studied by the detection of active oxygen and surface species in water, Phys. Chem. Chem. Phys. 17 (2015) 1–8.